Denervation-induced NRG3 aggravates muscle heterotopic ossification via the ErbB4/PI3K/Akt signaling pathway

LIN MA[1*], XIA KANG[2*], JINDONG TAN[1], YUNJIAO WANG[1], XIAO LIU[1], HONG TANG[1], LIN GUO[1], KANGLAI TANG[1] and XUTING BIAN[1,3]

[1]Department of Sports Medicine, Southwest Hospital, Army Medical University, Chongqing 400038, P.R. China; [2]Pancreatic Injury and Repair Key Laboratory of Sichuan Province, The General Hospital of Western Theater Command, Chengdu, Sichuan 610083, P.R. China; [3]Department of Health Service, Shigatse Branch, Xinqiao Hospital, Army Medical University, Shigatse 857000, Tibet Autonomous Region. P.R. China

Received April 17, 2024; Accepted August 14, 2024

DOI: 10.3892/mmr.2024.13374

Abstract. Peripheral nerve injury exacerbates progression of muscle heterotopic ossification (HO) and induces changes in expression of local cytokines in muscle tissue. The objective of the present study was to assess the impact of peripheral nerve injury on muscle HO development and the mechanism of cytokine modulation. A mouse model of gastrocnemius muscle HO was established and the sciatic nerve cut to simulate peripheral nerve injury. To evaluate the underlying factors contributing to the exacerbation of muscle HO resulting from denervation, fresh muscle tissue was collected and micro-computed tomography, histochemical staining, RNA-sequencing, reverse transcription-quantitative PCR, Western blot, muscle tissue chip array were performed to analyze the molecular mechanisms. Sciatic nerve injury exacerbated HO in the gastrocnemius muscle of mice. Moreover the osteogenic differentiation of nerve-injured muscle tissue-derived fibro-adipogenic progenitors (FAPs) increased *in vitro*. The expression of neuregulin 3 (NRG3) was demonstrated to be increased after nerve injury by muscle tissue chip array. Subsequent transcriptome sequencing analysis of muscle tissue revealed an enrichment of the PI3K/Akt pathway following nerve injury and an inhibitor of the PI3K/Akt pathway reduced the osteogenic differentiation of FAPs. Mechanistically, *in vitro*, peripheral nerve injury increased secretion of NRG3, which, following binding to ErbB4 on the cell surface of FAPs, promoted expression of osteogenesis-associated genes via the PI3K/Akt signaling pathway, thus contributing to osteogenic differentiation of FAPs. *In vivo*, inhibition of the PI3K/Akt pathway effectively protected against muscle HO induced by peripheral nerve injury in mice. The present study demonstrated that the regulatory roles of NRG3 and the PI3K/Akt pathway in peripheral nerve injury exacerbated muscle HO and highlights a potential therapeutic intervention for treatment of peripheral nerve injury-induced muscle HO.

Correspondence to: Dr Kanglai Tang or Dr Xuting Bian, Department of Sports Medicine, Southwest Hospital, Army Medical University, 30 Gaotanyan Street, Chongqing 400038, P.R. China
E-mail: tangkanglai2023@163.com
E-mail: anthonybean@163.com

*Contributed equally

Key words: heterotopic ossification, cytokine, muscle, signal transduction, bone remodeling

Introduction

Heterotopic ossification (HO) is a pathological process characterized by formation of bone within muscle, ligaments or other soft tissues (1,2). HO occurs after deep burn, fracture, total hip replacement, brain or medullary injury (3-5). Muscle HO is a form of HO characterized by abnormal formation of bone tissue within skeletal muscle, typically in response to trauma, surgery or other types of injury (6,7). This can result in joint dysfunction, as the presence of heterotopic bone within muscle tissue can cause pain, decreased range of motion and other complications (8).

The morbidity of HO following central neurological injury is 10 to 53% and the prevalence of genetic HO is extremely rare, affecting 1 in 2,000,000 people (9). While the condition can occur at all ages, it occurs most commonly in young adults, with the highest occurrence observed during 20-40 years old. Muscle HO does not appear to have a significant sex or racial or ethnic predilection (10). Muscle HO is hypothesized to involve a complex interplay of signaling pathways and cellular processes (11,12). The mechanisms underlying this process are not fully understood, but they may involve intricate interactions between inflammatory molecules, growth factors and other signaling pathways. Thus, better understanding of the pathogenesis of muscle HO could have implications for the development of novel treatments and therapies (13,14).

Peripheral denervation occurs when the nerve innervating a muscle is disrupted or severed, leading to loss of motor function and muscle atrophy. The peripheral nerves innervate muscles via neuromuscular junctions, which are synaptic connections established between motor neurons and muscles, as well as muscle sensory organs (15). While effects of denervation on muscle have been extensively studied (16-18), research has also

suggested a potential link between peripheral denervation and development of muscle HO (19). However, the mechanisms underlying the association between peripheral denervation and muscle HO are not fully understood. Better understanding of the effects of denervation on muscle HO could facilitate development of novel treatments and therapies for this condition and could help to elucidate the underlying pathophysiology.

Cytokines serve crucial functions in the regulation of inflammation and immune responses (20-22). The release of cytokines serves a role in the process of muscle degeneration and regeneration following denervation (23). Following denervation, the affected muscle tissue increases susceptibility of satellite cells to apoptosis, contributing to the inability of muscle to regenerate after prolonged periods without neural input. Loss of muscle mass is frequently associated with an increase in pro-inflammatory cytokines, as these are considered critical mediators of catabolic responses, such as muscle-specific protein break down (17). Moreover, inflammatory cells are involved in this process with a surrounding infiltration of cytokines, such as substance P and calcitonin gene related peptide (CGRP), from peripheral, sensory neurons. These cytokines exert direct effects on muscle cells, including promoting the degradation of muscle tissue and activation of muscle stem cells for both degenerative and regenerative processes (24).

Neuregulin 3 (NRG3) is a member of the neuregulin family of signaling molecules and serves a role in cellular processes such as cell proliferation, differentiation and migration. NRG3 is primarily expressed in the central nervous system, where it serves a role in development and function of the brain (25). NRG3 may also serve a role in the mechanisms of bone formation and ossification (26). Achilleos and Trainor (27) reported that NRG3 is expressed in osteoblasts that are responsible for bone formation and that the expression of NRG3 is increased during bone healing. Lazard *et al* (28) reported that NRG3 can promote the differentiation of mesenchymal stem cells into osteoblasts, which are responsible for formation of bone tissue.

Non-myogenic cells serve a role in skeletal muscle degeneration (29,30). In particular, fibro-adipogenic progenitors (FAPs) are regulators of muscle stem cell function and skeletal muscle degeneration (31,32). Previous studies have suggested that FAPs have the potential to differentiate into osteogenic or chondrogenic cells when exposed to specific conditions, such as bone morphogenetic protein-2 (BMP-2) (33-35). These findings suggest that FAPs are a cellular source of muscle HO. However, the association between denervation-induced changes in cytokine expression and muscle HO requires further assessment.

In the present study, a mouse model of gastrocnemius muscle HO was established and the sciatic nerve was cut to simulate peripheral nerve injury. The effect of peripheral nerve injury on muscle HO and underlying mechanism were assessed by detecting the changes in cytokine expression in muscle tissue and analyzing transcriptome-wide differential expression, along with *in vitro* experiments with FAPs.

Materials and methods

Experimental animals. A total of 90 C57BL/6 6-8 week-old male mice (weight, 20-25 g) were obtained from Army Medical University, Chongqing, China. All mice were housed in a pathogen-free and 60% humidity environment with free access to food and water. The temperature was maintained at 22-26˚C with a 12-h light/12-h dark cycle. All animal experimental procedures and euthanasia were approved by The Laboratory Animal Welfare and Ethics Committee of Third Military Medical University (Chongqing, China; approval no. AMUWEC20210782). At the end of the experiment, mice were euthanized by injection with 30 mg/kg pentobarbital sodium anesthetic injection followed by cervical dislocation. Heartbeat and breathing were checked to ensure successful euthanasia. Throughout the experiment, mice were assessed once/day for general indicators and once/week for specific indicators. When any mice demonstrated any of the humane end points, the animal experiment was terminated (Table SI). No mice died prior to the end of the study.

Study design. Left hindlimb intramuscular injection of cardiotoxin (CTX; 50 μl 10 μmol/l) was used to establish a muscle HO model. To assess the role of peripheral denervation in muscle HO, mice were randomly assigned to the following groups: i) CTX injection (CTX group) and ii) CTX injection with left hindlimb peripheral denervation group (CTX-DeN group). To assess the role of NRG3/ErbB4 signaling in muscle HO, mice were randomly assigned to the following groups: i) CTX-DeN and ii) CTX-DeN + 10 mg/kg dacomitinib. Finally, micro-computed tomography (micro-CT), PCR and cytokine chip analyses were performed to assess the degree of HO.

Surgical procedure. The peripheral denervation model was established according to Akhter *et al* (36) as follows: Mice were administered 30 mg/kg pentobarbital sodium anesthetic injection in the right lower abdomen. The mice were placed on a sterilized area for preparation of the hindlimb, which was secured in an extended position with surgical tape. The skin was palpated to identify the femur and a small incision (<2 cm) was made 2 mm medially in the skin with a fine scalpel. The biceps femoris was blunt dissected at mid-thigh level using scissors, exposing the sciatic nerve, which was carefully isolated from connective tissue and cut with micro-scissors. After ensuring there was no excessive bleeding, the wound was closed (CTX-DeN group). Mice in the CTX group underwent the same procedure except for the cutting of sciatic nerve. After peripheral denervation surgery, 50 μl 10 μmol/l CTX (cat. no. C9759; MilliporeSigma) was injected into both calf muscles of each mouse. A gelatin sponge (cat. no. 20153141505; JinLing Pharmaceutical) was sectioned 1 mm thick discs and 5 μl aliquots containing 0.5 μg of recombinant BMP-2 (cat. no. Z02913; GenScript.) was adsorbed onto each disc. The medial surface of the calf muscles in the leg was incised longitudinally. A single disc containing BMP-2/gelatin was inserted intramuscularly. The disc was implanted between the gastrocnemius and soleus muscles around the CTX injection site. Finally, the skin was sutured closed. In the CTX-DeN + dacomitinib group, 1 day after the animal model was established, a single perimuscular injection of 10 mg/kg dacomitinib (20 nM, dissolved in DMSO; 20 μl) was administered around the gelatin implantation site (37).

Cell isolation and fluorescence-activated cell sorting. The isolation of FAPs was conducted as described in a previous

study (38). Muscles were obtained from both hind limbs of mice. Non-muscle tissue was excised and finely minced. Subsequently, enzymatic digestion was performed using 0.2% type II collagenase (cat. no. LS004176; Worthington Biochemical Corporation) for 1 h at 37˚C. The resulting muscle plasma was filtered through cell filters with pore sizes of 100 and 40 μm (cat. nos. 431752 and 431750, respectively; BD Biosciences). Red blood cell lysis buffer (cat. No. C3702, BD Bioscience) was utilized to eliminate red blood cells, and the cells were resuspended in PBS wash buffer containing 2% FBS (Cat. No. SH30406.05, HyClone) and stained with antibodies for 30 min at 4˚C in the absence of light. The gating strategy for flow cytometry involved $CD31^-$, $CD45^-$, Integrin $\alpha7^-$, stem cell antigen-1^+ ($Sca\text{-}1^+$) and Platelet Derived Growth Factor Receptor $Alpha^+$ ($PDGFR\alpha^+$) cells. The antibodies used included Alexa Fluor 488-CD31 (1:100, Cat. No. 160,208, Biolegend), Alexa Fluor 488-CD45 (1:100, Cat. No. 160,306, Biolegend), APC-Integrinα7 (1:100, Cat. No. FAB3518A, R&D), APC-Cy7-Sca-1 (1:100, Cat. No. 108,126, Biolegend) and biotin-PDGFRα (1:100, Cat. No. AF1062, R&D). The stained cells were analyzed using FACSAria III (BD Biosciences, NJ, USA). The data was analysed by using FlowJo v10 (Flowjo, LLC., OR, USA).

Cell culture. Primary FAPs were cultured on Matrigel-coated tissue culture plates (Cat. No. CLS430639, Corning, Inc.) in DMEM (Cat. No. SH30243.01B, HyClone) supplemented with 20% fetal bovine serum (Cat. No. SH30406.05, HyClone), 1% penicillin-streptomycin and 2.5 ng/ml basic fibroblast growth factor (cat. no. PHG0021; Invitrogen; Thermo Fisher Scientific, Inc.) at 37˚C. The medium was replaced with fresh medium after 3 days. To induce osteogenic differentiation, cells were treated with osteogenesis induction medium (cat. no. HUXMX-90021; Cyagen Biosciences, Inc.) at 37˚C in a saturated humidity incubator containing 5% CO_2 for 14 days; medium was replaced every 3 days. To verify osteogenic differentiation of FAPs via the PI3K/Akt signaling pathway, FAPs were cultured in vitro and divided into four groups as follows: i) normal medium; ii) osteogenic-inducible medium (OIM); iii) OIM + NRG3 (2.0 μg/ml, cat. no. ab276716, Abcam) and iv) OIM + NRG3 (2.0 μg/ml) + 1 μM dacomitinib. After 14 days of culture, Alizarin Red S staining was performed.

Micro-CT. Following euthanasia, mouse hindlimbs were imaged by micro-CT (vivaCT, Skyscan 1276, Bruker) to detect HO formation at 4 weeks post-surgery. The scanner was configured with a voltage of 60 kV and pixel resolution of 10 μm. Once the scans were complete, the images were reconstructed, which allowed visualization and analysis of the 3D microstructure of the hindlimbs. The results were analyzed using Scanner software (3D.Suite, SKYSCAN 1276, Bruker) for Micro-CT. Bone mineral density (BMD) were measured.

Histochemical staining. The fresh frozen muscle tissue was sectioned into 8-μm slices using a cryostat and fixed with 4% PFA at 4˚C for 5 min. Muscle histology was assessed by hematoxylin-eosin (H&E) staining (Beijing Solarbio Technology Science & Technology Co., Ltd.). Slices were stained for 5 min in hematoxylin and 2 min eosin solution at 24˚C before being dried and sealed with neutral gum. The cells were fixed with 4% PFA for 10 min at 4˚C and subsequently rinsed in water and 60% isopropanol, prior to Alizarin Red S staining. After staining the cells with Alizarin Red S for 30 min at 24˚C, they were again rinsed in water. The positive-stanined cells of Alizarin Red S were counted manually. All the stained sections and cells were viewed and photographed under a Zeiss (Oberkochen) fluorescence Axiovert microscope equipped with a Zeiss AxioCam digital colour camera connected to the Zeiss AxioVision 3.0 system (magnification, 40).

RNA-sequencing (seq). For RNA-seq analysis of mouse hindlimbs. total RNA was extracted from tissue samples using TRIzol (Cat. No. 15596026, Invitrogen). Subsequently, total RNA was qualified and quantified using a Fragment Analyzer or Agilent 2100 Bioanalyzer (Agilent, CA, USA). Following addition of a single 'A' base and ligation of the adapter to cDNA fragments, PCR was employed for the final cDNA library creation using Optimal Dual-mode mRNA Library Prep kit(cat. no. LR00R96, BGI). RNA was processed to generate a cDNA library, which was subjected to high-throughput sequencing using a new-generation sequencing platform (input 1 pM for DNA sequencing) using MGISEQ-2000RS High-throughput Sequencing Set (cat. no. FCL SE50) (60 cycles; Cat. No. 1000006138, MGI). The DNBs are loaded into the patterned nanoarray and SE 50 (Single-end for direction of sequencing, and 50 bp for length) bases reads are generated on BGISEQ platform (BGI-Shenzhen, China). Subsequently, Dr. Tom multi-omics data mining system (https://biosys.bgi.com) was used for data analysis, mapping and mining. HISAT2 (v2.1.0) software was used to align clean data to the reference genome for differential gene analysis. We used the DESeq2 (version 1.4.5) for differential gene detection with a condition of Q value ≤ 0.05 or FDR ≤ 0.001. Hypergeometric test based on the Phyper (https://en.wikipedia.org/wiki/Hypergeometric_distribution) function to perform GO (geneontology.org/) and KEGG (kegg.jp/) enrichment analysis on the differential genes, with Qvalue ≤ 0.05 as the threshold.

Reverse transcription-quantitative PCR (RT-qPCR) analysis. Total RNA was extracted from mouse hindlimbs using TRIzol reagent (cat. no. 15596026, Invitrogen; Thermo Fisher Scientific, Inc.). RNA was reverse-transcribed into cDNA using the RevertAid First Strand cDNA Synthesis kit (cat. no. K1622, Thermo Fisher Scientific, Inc.) according to the manufacturer's instructions. A reaction system containing primers, dNTP and buffer was prepared using an ABI 7500 Real-Time PCR system (Applied Biosystems; Thermo Fisher Scientific, Inc.). The amplification reaction was performed in a thermal cycler using a SYBR kit (cat. no. RR4420L, Takara Bio, Inc.). Thermocycling conditions included incubation at 95˚C for ten seconds, followed by 40 cycles of 95˚C for five sec and 60˚C for 30 sec. Relative gene expression was quantified by densitometry and normalized to the expression of GAPDH). Amplification results were analyzed and quantified using the $2^{-\Delta\Delta Cq}$ method (39). The primer sequences used for PCR are listed in Table SII.

Western blotting. Total protein from FAPs was extracted using RIPA lysis buffer (cat. no. P0013P, Beyotime) and

quantified using a BCA kit (cat. no. P0010, Beyotime) and 50 μg protein/lane was separated by 10% SDS-PAGE (cat. no. 1620177; Bio-Rad Laboratories, Inc.), and the separated proteins were transferred to polyvinylidene difluoride membranes. The separated proteins were transferred onto a membrane. Membranes were incubated overnight at 4˚C in PBS containing 5% BSA (cat. no. BS114, Biosharp) with primary antibodies anti-PI3K (1:2,000; cat. no. bs-5570R, BIOSS), anti-phosphorylated (p)-PI3K (1:2,000; cat. no. bs-5538P, BIOSS), anti-AKT (1:2,000; cat. no. 10176-2-AP, Proteintech), anti-p-AKT (1:2,000; cat. no. 66444-1-Ig, Proteintech) and GAPDH (1:5,000; cat. no. 60004-1-Ig, Proteintech). Following primary incubation, membranes were incubated with goat anti-rabbit IgG secondary antibody (1:2,000; cat. no. SA00001-2,Proteintech) for 1 h at ambient temperature. Protein bands were stimulated with ECL kit (cat. no. WBULS0500, Millipore) and detected with a Bio-Rad ChemiDoc MP System (170-8280; Bio-Rad Laboratories, Inc.). ImageJ software (version 1.46r, National Institutes of Health) was used to analyse the results.

Muscle tissue chip array. Muscles were obtained from hind limbs of mice at 4 weeks after modeling. Non-muscle tissue was carefully excised and finely minced. The experiment was performed using the Raybiotech reagent kit (Wayen Biomedical Technology) and was conducted according to the standard operating procedures of Raybiotech chip. Fresh muscle tissue culture supernatant was harvested and stored at -80˚C. Muscle tissue chips (AAM-BLG-308, Raybiotech) were obtained from Shanghai Wayen Biomedical Technology Co. Ltd. Agilent SureScan Dx Microarray Scanner chip scanner to scan the chip at 532 nm, Power (100%) conditions. The fluorescence signal intensity, which is then normalised after the data is read and generally analysed using the FI of the fluorescence signal with the background removed (F532 Median-B532 Median).

STRING database analysis of NRG3. By means of the STRING database (*version 12.0,* www.string-db.org/), we constructed the protein-protein interaction (PPI) network for NRG3. A network type of full STRING network with high confidence (minimum required interaction score=0.7) was selected.

Statistical analysis. Data are presented as the mean ± SD of ≥3 experimental repeats. Unpaired t test was used for comparisons between two groups. One-way analysis of variance with Tukey's post hoc test was used for comparisons between multiple groups. Model assumptions were checked using the Shapiro-Wilk normality test and Levene's test for homogeneity of variance and by visual inspection of residual and fitted value plots. $P<0.05$ was considered to indicate a statistically significant difference. Statistical analysis was performed using SPSS 26.0 software (IBM Corp.). Pearson correlation coefficients of gene expressions between each two samples were calculated.

Results

Denervation leads to more severe HO of muscle. To assess the effect of denervation on muscle HO, a model of muscle HO was established by CTX-DeN, with a sham surgical treatment performed in the control group. Micro-CT was performed 4 weeks post-surgery (Fig. 1A). The BMD in the CTX-DeN group (0.780±0.020 g/cm^3) was significantly increased compared with CTX group (0.479±0.032 g/cm^3) (Fig. 1B), indicating a higher degree of HO in the denervated group compared with the control. H&E staining demonstrated that the CTX-DeN group had a significantly higher HO ratio compared with the CTX group (Fig. 1C and D). RT-qPCR was performed on muscle tissue to assess osteogenesis-related gene expression. mRNA levels of osteopontin (OPN), RUNX2, osterix/SP7 (encoded by the SP7 gene, SP7), alkaline phosphatase (ALPL) and bone morphogenetic protein-2 (BMP2) were significantly higher in the CTX-DeN group compared with the CTX group (Fig. 1E). These results suggested that denervation led to increased HO of muscles.

Denervation increases secretion of NRG3 and NRG3 is most closely associated cell membrane surface receptor was ErbB4. To assess the underlying factors contributing to exacerbation of muscle HO resulting from denervation, fresh muscle tissue was collected and the levels of 15 cytokines were quantified. The protein level of NRG3 was increased in the CTX-DeN group compared with the CTX group (Fig. 2A; Table SIII), suggesting that denervation led to an increase in the secretion of the cytokine NRG3 in muscle tissue. To determine the mechanism of how increased NRG3 secretion affects HO, we constructed the protein-protein interaction (PPI) network for NRG3 by means of the STRING database (version 12.0). A network type of full STRING network with high confidence (minimum required interaction score=0.7) was selected. The STRING database was used for protein interaction network visualization and predicted the molecular interactions of NRG3. This predicted that the most closely associated cell membrane surface receptor was ErbB4 (Fig. 2B). RT-qPCR was used to measure the levels of ErbB4 mRNA in muscle tissue and demonstrated that the expression of ErbB4 was significantly higher in the denervated group compared with the control (Fig. 2C). This suggested that denervation may exert its effects through upregulating the release of NRG3 in muscle tissue and binding to ErbB4 receptors, thereby contributing to the exacerbation of HO.

Ossification and cartilage development-associated genes are enriched in denervation-aggravated muscle HO. To assess how denervation causes exacerbation of muscle HO, transcriptome sequencing was performed on muscle tissue (Fig. S1). The results demonstrated a total of 1,066 differentially expressed genes, of which 752 were upregulated and 314 genes were downregulated in the CTX-DeN group compared with the CTX group (Fig. 3A and Fig. S2). Gene Ontology functional enrichment analysis of differentially expressed genes reported that biological processes, including 'ossification' and 'cartilage development' were significantly enriched (Fig. 3B-D). Freshly sorted FAPs were cultured in osteogenic induction medium for 14 days. Alizarin Red S staining was performed. The number of positively stained cells from the CTX-DeN group was significantly increased compared with the CTX group (Fig. 3E and F).

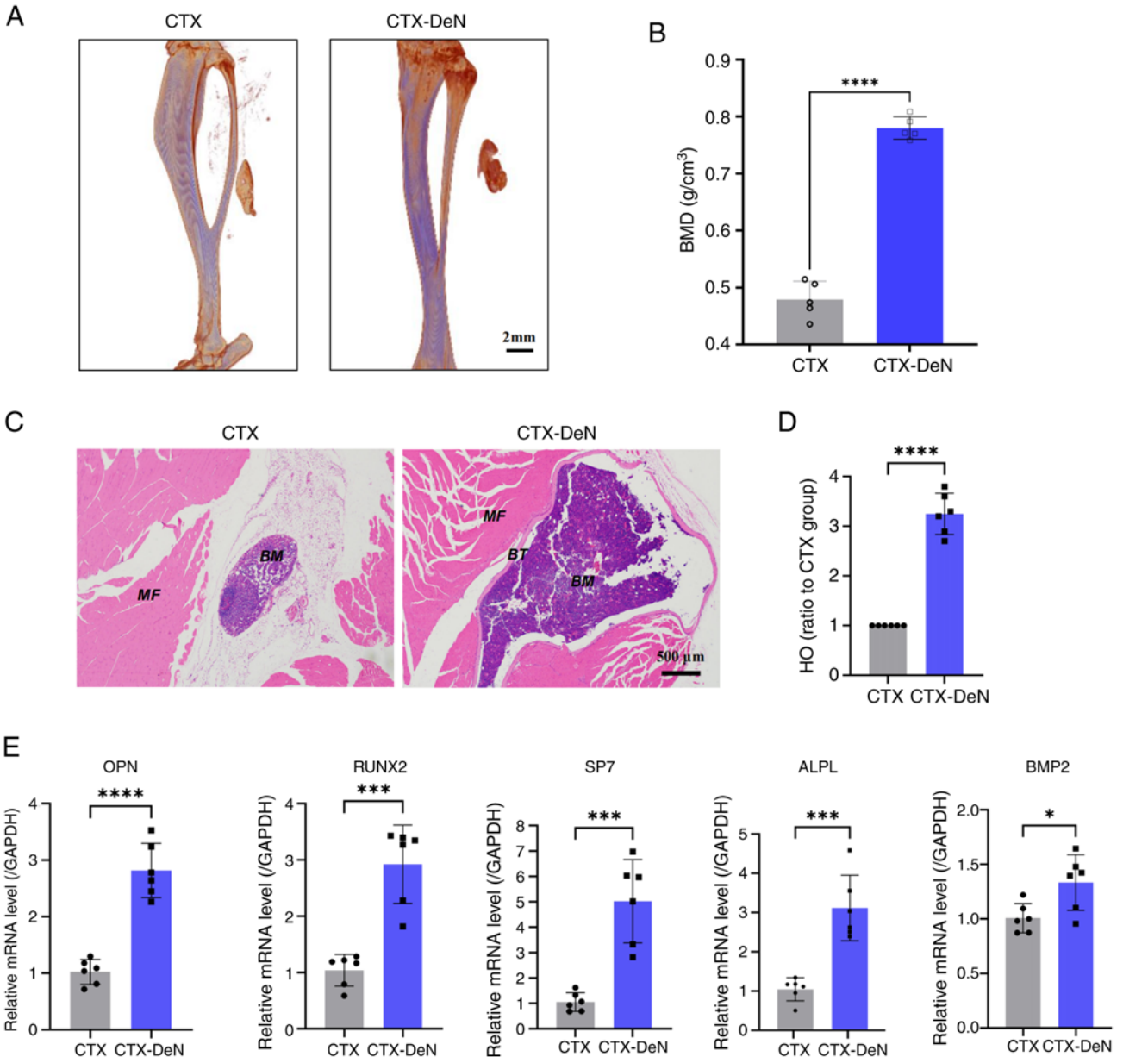

Figure 1. Denervation leads to increased HO of calf muscles. (A) Morphology of muscle HO was scanned by micro-computed tomography. (B) BMD was subjected to statistical analysis. (C) Calf muscle was subjected to hematoxylin-eosin staining. (D) HO ratio to CTX. (E) RT-qPCR analysis of gene expression levels of OPN, RUNX2, SP7, ALPL and BMP2. *P<0.05, ***P<0.005 and ****P<0.001. CTX, cardiotoxin; DeN, denervation; MF, Muscle fiber; BT, Bone tissue; BM, Bone mineral; OPN, Osteopontin; SP7, Osterix/SP7 (encoded by the SP7 gene); ALPL, Alkaline phosphatase; BMP2, Bone morphogenetic protein-2; HO, heterotopic ossification; BMD, bone mineral density; RT-qPCR, reverse transcription-quantitative PCR.

NRG3 affects osteogenic differentiation of FAPs via the PI3K/Akt signaling pathway. To assess the role of NRG3/ErbB4 signaling on the PI3K/Akt signaling pathway in HO exacerbation, dacomitinib, an inhibitor of ErbB4 was used. Osteogenic induction medium increased the number of Alizarin Red S stained cells in OIM group was more than DMEM group; this was enhanced by addition of NRG3. Following addition of dacomitinib, osteogenic differentiation of FAPs was inhibited, and the number of Alizarin Red S stained cells in OIM+NRG3+dacomitinib group was less than OIM+NRG3 group (Fig. 4A and B). RT-qPCR analysis of osteogenesis-associated genes was consistent with results of alizarin Red S staining. The mRNA level of RUNX2 in OIM group was more than DMEM group, and the mRNA level of RUNX2 in OIM+NRG3 group was more than OIM group. Following addition of dacomitinib, the mRNA level of RUNX2 in OIM+NRG3+dacomitinib group was less than OIM+NRG3 group (Fig. 4C). KEGG pathway enrichment analysis was performed on differentially expressed genes; a number of pathways, including 'protein digestion and absorption' were enriched. Based on previous literature (40,41) and the results of KEGG, the PI3K/Akt signaling pathway associated with osteogenesis was screened (Fig. 4D). Western blotting of PI3K/Akt pathway-associated proteins demonstrated that the protein expression levels of p-PI3K and p-Akt were significantly increased in the OIM group compared with DMEM group and OIM + NRG3 group compared with the OIM group. Moreover, in the OIM + NRG3 + dacomitinib group,

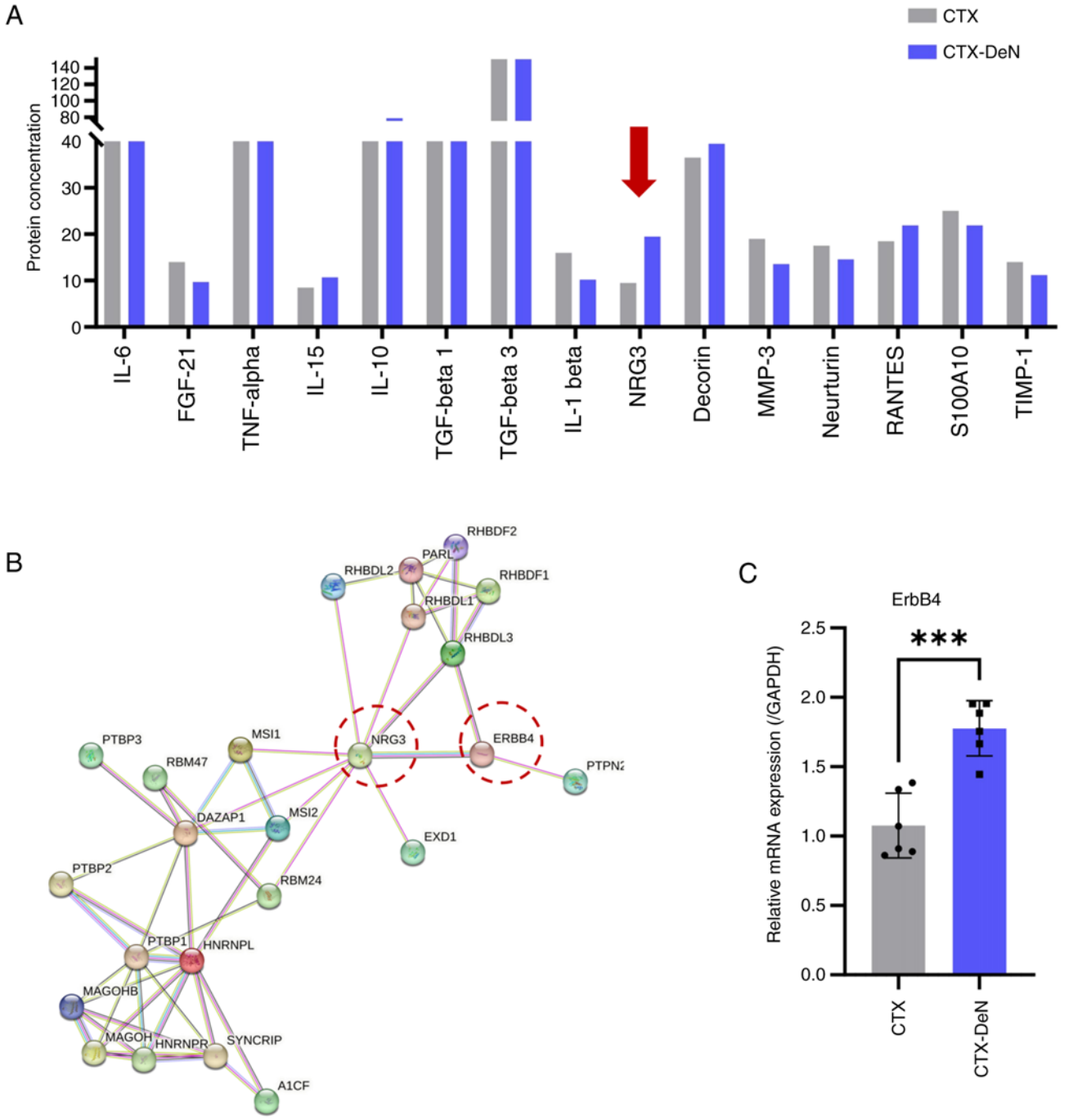

Figure 2. DeN increases secretion of NRG3. (A) Cytokine microarray analysis was used to quantify the levels of cytokine secretion in muscle heterotopic ossification. Arrow indicates the protein level of NRG3 was increased most in the CTX-DeN group compared with the CTX group. (B) Molecular interactions of NRG3. (C) Reverse transcription-quantitative PCR analysis of ErbB4 mRNA levels. n=6/group. ***P<0.005. NRG3, Neuregulin 3; CTX, Cardiotoxin; FGF, Fibroblast growth factor; TGF, Transforming growth factor; RANTES, Regulated upon activation normal T cell expressed and presumably secreted; S100A10, p11, annexin II light chain, calpactin light chain; TIMP, The tissue inhibitors of matrix metalloproteinases; DeN, Denervation.

protein expression levels of p-PI3K and p-Akt were decreased compared with the OIM + NRG3 group (Fig. 4E and F).

Dacomitinib attenuates denervation-aggravated HO of muscle. Finally, to confirm the mechanistic findings at the cellular level, a muscle HO model was re-established in the mouse gastrocnemius muscle. Micro-CT demonstrated that the BMD of the CTX-DeN + dacomitinib group (0.533±0.036 g/cm^3) was significantly decreased compared with the CTX-DeN group(0.802±0.046 g/cm^3) (Fig. 5A and B).

Discussion

The association between peripheral nerves and development of muscle HO has been demonstrated (42) but the relationship with the progression of muscle HO is unclear. The understanding of the association between the peripheral nerves and the progression of muscle HO may serve as a diagnostic guide and aid in selecting an appropriate treatment modality. The current treatment for extensive injury-induced HO is surgical excision (43). However, certain patients may not be suitable

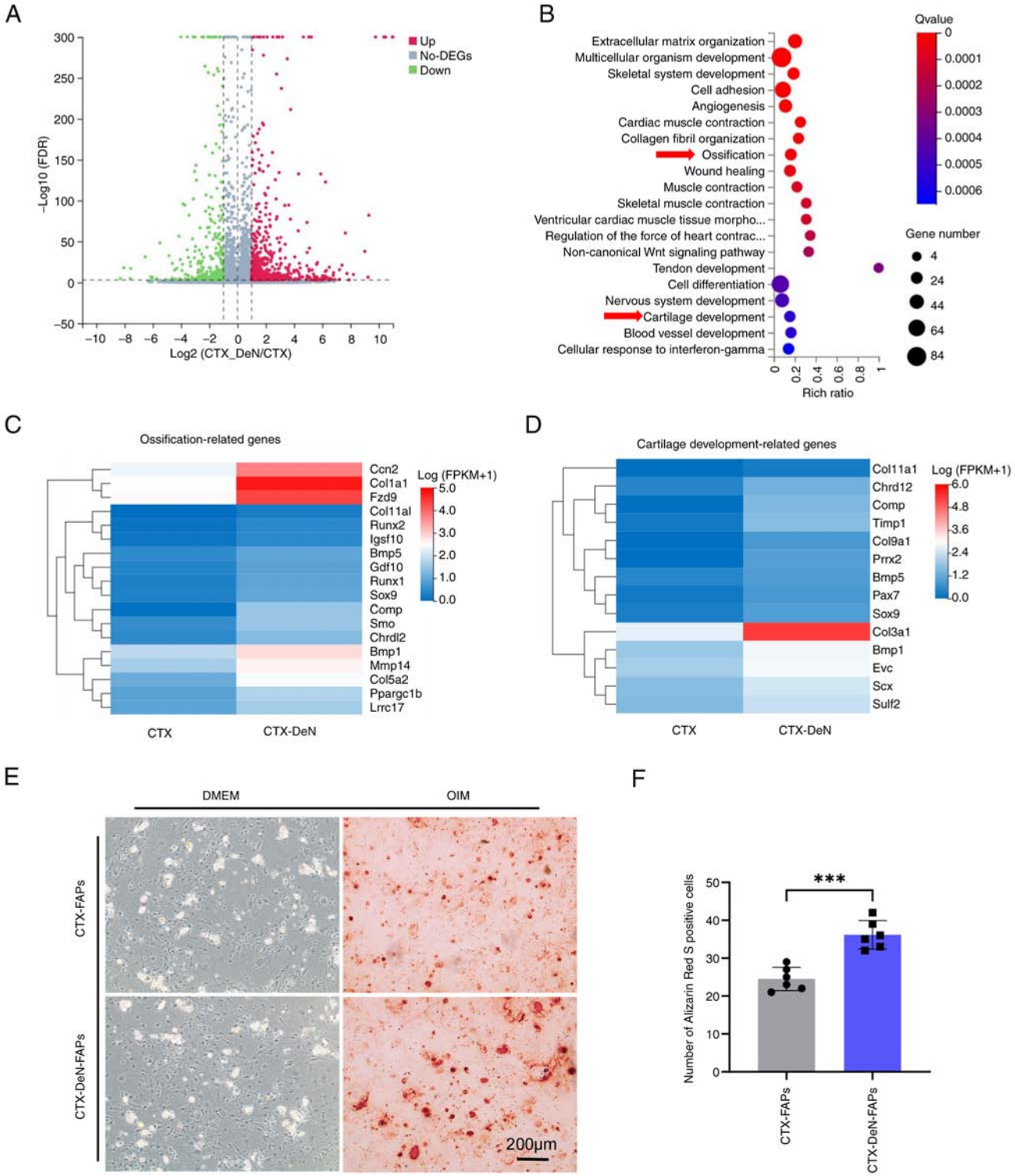

Figure 3. DeN-aggravated muscle heterotopic ossification. (A) A total of 1066 differentially expressed genes, of which 752 genes were upregulated and 314 genes were downregulated in the CTX-DeN group compared with the CTX group. (B) Gene Ontology functional enrichment analysis of differentially expressed genes reported that biological processes. Arrows indicate enriched. (C) In the CTX-DeN group, 'ossification-related genes' was significantly enriched compare with CTX group. (D) In the CTX-DeN group, 'cartilage development-related genes' was significantly enriched compare with the CTX group. (E) Alizarin red staining and (F) quantification of induced osteogenic differentiation of fibro-adipogenic progenitors *in vitro*. n=6/group. ***P<0.005. DeN, denervation; CTX, Cardiotoxin; FDR, False Discovery Rate; DEG, Differentially expressed genes; FPKM, Fragments Per Kilobase of exon model per Million mapped fragments; OIM, Osteogenic-inducible medium.

candidates for complete excision due to the nature or location of ossification. Furthermore, the possibility of HO recurrence after surgery exists (44), accompanied by associated procedural risks such as infection and neurovascular injury. Improving understanding of the underlying mechanisms of pathological bone formation may facilitate the development of strategies aimed at preventing unwanted ossification while using its regenerative potential for applications in tissue

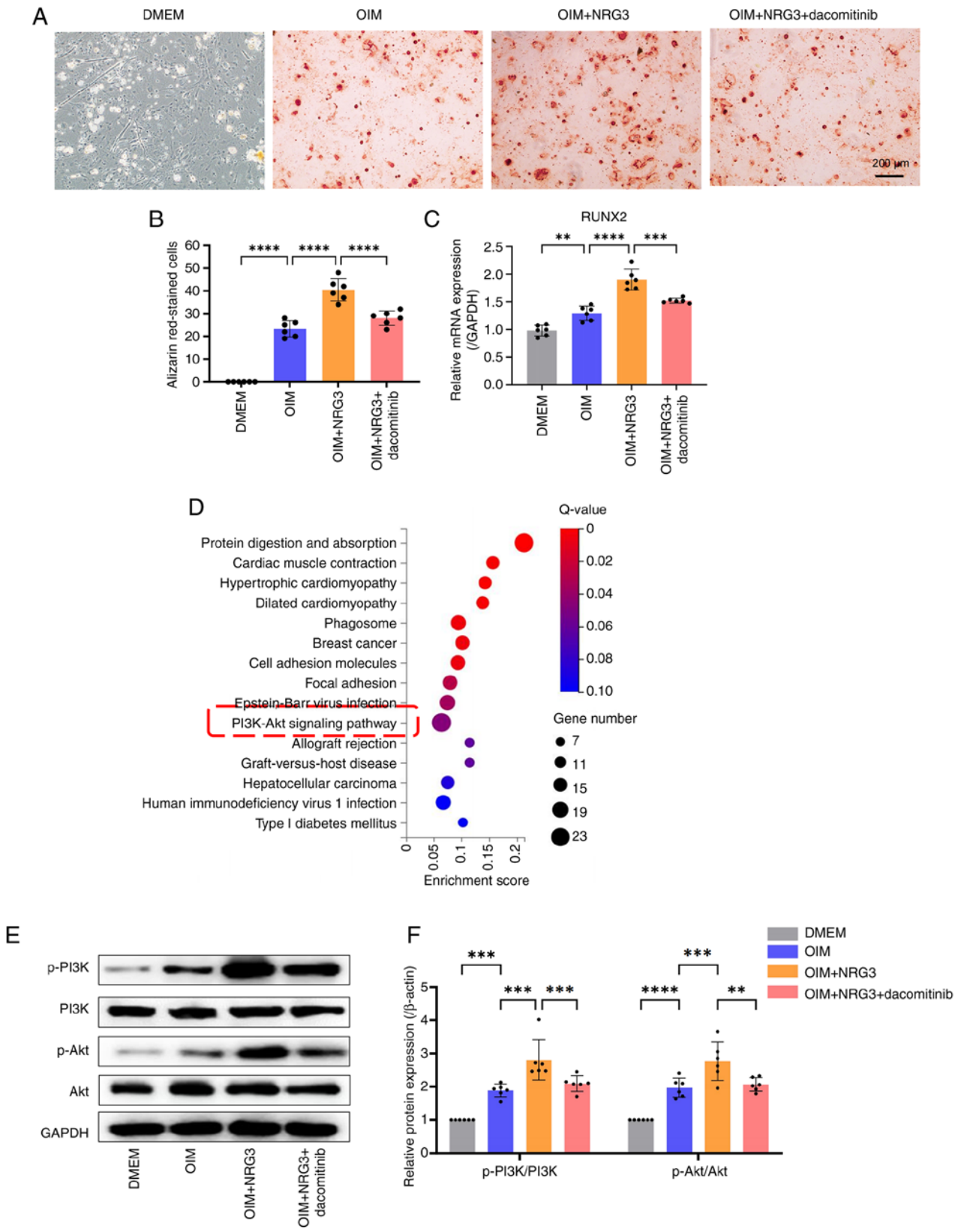

Figure 4. NRG3 affects osteogenic differentiation of FAPs via the PI3K/Akt signaling pathway. (A) Alizarin red staining and (B) quantification of induced osteogenic differentiation of FAPs cells *in vitro*. (C) Reverse transcription-quantitative PCR analysis of mRNA expression levels of RUNX2. (D) Enrichment of Kyoto Encyclopedia of Genes and Genomes pathway in transcriptome sequencing. (E) Western blotting of PI3K/Akt signaling pathway-associated (F) protein expression during osteogenic differentiation of FAPs *in vitro*. n=6/group. **P<0.05, ***P<0.01 and ****P<0.001. NRG3, neuregulin 3; FAP, Fibro-adipogenic progenitors; OIM, Osteogenic-inducible medium; p, Phosphorylation.

engineering systems (45). In the present study, a mouse model of gastrocnemius muscle HO was established by injury to the sciatic nerve; imaging and histological observation demonstrated that peripheral nerve injury promoted progression

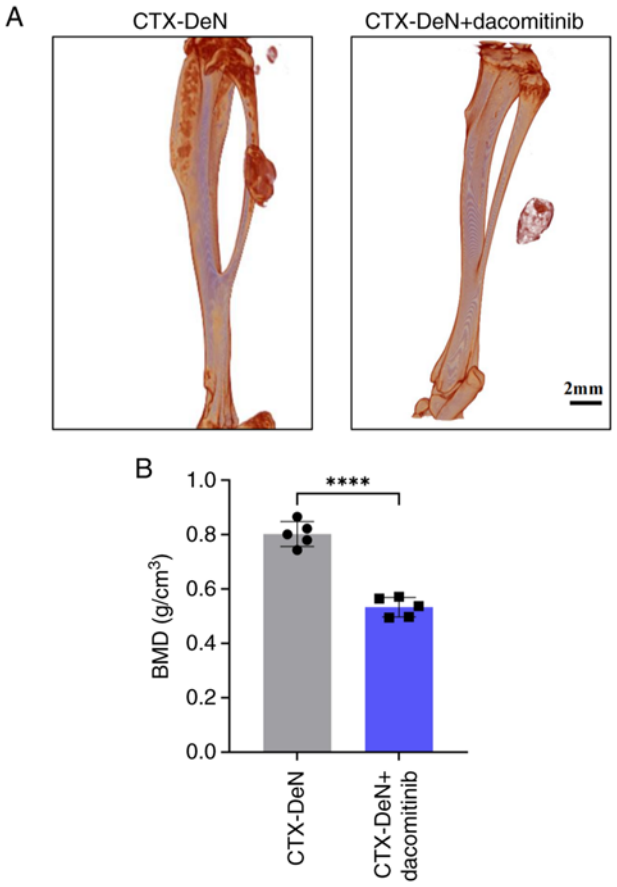

Figure 5. Dacomitinib alleviates ectopic ossification caused by denervation. (A) Morphology of muscle heterotopic ossification was observed by micro-computed tomography and (B) BMD was assessed. n=5/group. ****P<0.001. BMD, bone mineral density; CTX, Cardiotoxin; DeN, Denervation.

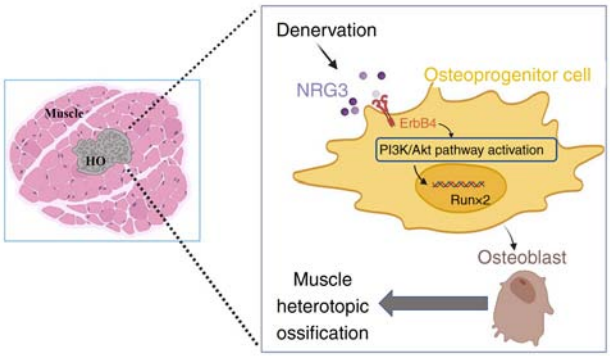

Figure 6. Peripheral nerve injury exacerbated progression of muscle HO, caused by the release of NRG3, which induced osteogenic differentiation of FAPs via the ErbB4/PI3K/Akt signaling pathway. NRG3, Neuregulin 3. HO, heterotopic ossification.

of muscle HO. This is not only consistent with the findings of Qureshi *et al* (46) and Olmsted-Davis *et al* (47) but also increases the knowledge of the association between peripheral nerve injury and development of muscle HO and clarifies the relationship between peripheral nerve injury and progression of muscle HO.

Increased expression of BMP-2 caused by damage to the neurovascular barrier due to neuroinflammation is hypothesized to be the mechanism by which peripheral nerve damage leads to muscle HO (48-50). In the present study, a mouse model of gastrocnemius muscle HO was established by CTX injection, based on previous literature reports (51-53), and locally applied gelatin solution saturated with BMP-2 to increase the formation of ectopic bone. Denervation leads to more severe HO of muscle and increases the formation of HO (51). The levels of cytokines in HO muscle tissue were measured to determine their involvement in the progression of HO. The expression levels of multiple cytokines, including NRG3, were altered after peripheral nerve injury. Based on analysis of absolute and differential expression, NRG3 may serve a role in progression of muscle HO due to peripheral nerve injury.

The activation of FAPs cells occurs following muscle trauma. Previous research primarily focused on understanding intracellular signaling pathways involved in wound repair (54). To the best of our knowledge, however, there is a lack of research regarding upstream mediators and mechanisms regulated by muscle innervation that govern FAP recruitment, expansion and differentiation (54). Gallardo *et al* (55) developed a denervation mouse model and reported activation of Yes-associated protein 1/(transcriptional co-activator with PDZ-binding motif) TAZ signaling in FAPs, suggesting their involvement in FAP activation, proliferation and differentiation. In the present study, using FAPs as a model of muscle tissue, FAPs underwent significant osteogenic differentiation upon induction of NRG3. This suggested that FAPs may a cellular source of muscle HO. As non-myogenic cells, FAPs serve a role in muscle injury repair, especially in skeletal muscle degeneration and regeneration (38). Previous studies (34,56) have reported that FAPs exhibit osteogenic or chondrogenic differentiation under specific culture conditions in the presence of BMP-2. Intramuscular transplantation of FAPs combined with Matrigel and BMP-2 has demonstrated that these cells form cartilage and calcium deposits *in vivo* (33). Lineage tracing using PDGFRα^{-} mice reported that the majority of osteoblasts in BMP-2-induced *in vivo* HO are derived from FAPs (35). These findings suggest that FAPs have multilineage differentiation potential and serve a role in muscle HO.

The present study demonstrated through *in vitro* and *in vivo* experiments that NRG3 modulated the PI3K/Akt pathway, which induced osteogenic differentiation of FAPs via binding to ErbB4 through protein-protein interaction network by STRING database. NRG3 activates ErbB receptors, including ErbB2, ErbB3 and ErbB4. Upon binding to its receptor, NRG3 initiates downstream signaling pathways, such as the PI3K/Akt and mitogen-activated protein kinase pathways, which serve roles in cellular processes including survival, proliferation and differentiation (57). This was supported by results of KEGG pathway enrichment analysis of the transcriptome sequencing data. These results suggested that the cytological cause of the exacerbation of denervation-induced muscle HO may be increased secretion of NRG3 and binding to ErbB4, thus activating the PI3K/Akt pathway, leading to increased expression of genes related to osteogenic differentiation (Fig. 6). Fisher *et al* (58) suggested that ErbB signaling serves a role in bone formation and ossification. ErbB2 and ErbB3 are expressed in osteoblasts, which are bone-forming

cells involved in regulation of differentiation and proliferation of periosteal cells. Furthermore, Linder *et al* (59) reported that activation of the ErbB receptor family by specific ligands can promote bone formation and mineralization. In the present study, C57BL/6 mice were used as animal models due to genetic and physiological similarity to humans. The age of 8-12 weeks in mice corresponds to ~20 years of age in humans, as they have fully developed but have not yet been affected by aging (51-53).

Dacomitinib is a reversible pan-epidermal growth factor receptor (EGFR) inhibitor (60), which selectively targets EGFR, and is an irreversible inhibitor of three ErbB family kinase members (ErbB1, ErbB2, and ErbB4) (61). Dacomitinib decreased osteogenic differentiation of FAPs was reduced. Western blotting of PI3K/Akt pathway-associated proteins demonstrated expression levels of p-PI3K and p-Akt significantly increased in the OIM + NRG3 group compared with the OIM group. Moreover, in the OIM + NRG3 + dacomitinib group, protein expression levels of p-PI3K and p-Akt were decreased compared with the OIM + NRG3 group. These results suggested that denervation led to osteogenesis-related biological processes in muscle tissue and the PI3K/Akt signaling pathway may mediate this process. The aforementioned results suggested that increased secretion of NRG3, through binding to ErbB4, activates the PI3K/Akt pathway, leading to increased expression of genes related to osteogenic differentiation and exacerbation of denervation-induced muscle HO. Dacomitinib may serve as a potential treatment option for muscle HO.

A limitation of the present study is that FAPs were not confirmed as a cellular source of muscle HO. ErbB4 inhibitor dacomitinib was used to suppress the signaling of NRG3/ErbB4, however, there may be other potential effects of this inhibitor. To the best of our knowledge, the impact on proliferation of FAPs has not been investigated. Future research should address this knowledge gap. Cell tracing should be used to confirm that FAPs are the cellular source of heterotopic calcification and gene knockout mice should be used.

In summary, the present study demonstrated that peripheral nerve injury exacerbated progression of muscle HO, potentially via increased expression of BMP-2 caused by the release of cytokine NRG3, which induced osteogenic differentiation of FAPs via the ErbB4/PI3K/Akt signaling pathway.

Acknowledgements

Not applicable.

Funding

The present study was supported by the Key Projects of the Natural Science Foundation of China (grant no. 82130071).

Availability of data and materials

The data generated in the present study may be found in The National Center for Biotechnology Information database under accession number PRJNA1136075 or at the following URL: ncbi.nlm.nih.gov/sra/PRJNA1136075.

Authors' contributions

LM, XK, KT, XL, YW, LG and XB conceived the study. LM and JT performed experiments. LM, LG, HT and XK designed the methodology. LM, YW, XL and HT collected data. JT, LM, YW, XL, KT and XB analyzed data. LM, JT, YW, XL and HT wrote the manuscript. LG, KT, XK and XB revised the manuscript. LM, KT and XB confirm the authenticity of all the raw data. All authors have read and approved the final manuscript.

Ethics approval and consent to participate

All animal experimental procedures were approved by The Laboratory Animal Welfare and Ethics Committee of Third Military Medical University (Chongqing, China; approval no. AMUWEC20210782).

Patient consent for publication

Not applicable.

Competing interests

The authors declare that they have no competing interests.

References

1. Edwards DS and Clasper JC: Heterotopic ossification: A systematic review. J R Army Med Corps 161: 315-321, 2015.
2. Ranganathan K, Loder S, Agarwal S, Wong VW, Forsberg J, Davis TA, Wang S, James AW and Levi B: Heterotopic Ossification: Basic-Science principles and clinical correlates. J Bone Joint Surg Am 97: 1101-1111, 2015.
3. Sturbois-Nachef N, Gatin L, Salga M, Geffrier A, Fontaine C and Allart E: Neurogenic heterotopic ossification in the upper limb. Hand Surg Rehabil 41S: S167-S174, 2022.
4. Reichel LM, Salisbury E, Moustoukas MJ, Davis AR and Olmsted-Davis E: Molecular mechanisms of heterotopic ossification. J Hand Surg Am 39: 563-566, 2014.
5. Nauth A, Giles E, Potter BK, Nesti LJ, O'brien FP, Bosse MJ, Anglen JO, Mehta S, Ahn J, Miclau T and Schemitsch EH: Heterotopic ossification in orthopaedic trauma. J Orthop Trauma 26: 684-688, 2012.
6. Moore-Lotridge SN, Li Q, Gibson BHY, Martin JT, Hawley GD, Arnold TH, Saito M, Tannouri S, Schwartz HS, Gumina RJ, *et al*: Trauma-Induced nanohydroxyapatite deposition in skeletal muscle is sufficient to drive heterotopic ossification. Calcif Tissue Int 104: 411-425, 2019.
7. Ji Y, Christopherson GT, Kluk MW, Amrani O, Jackson WM and Nesti LJ: Heterotopic ossification following musculoskeletal trauma: Modeling stem and progenitor cells in their microenvironment. Adv Exp Med Biol 720: 39-50, 2011.
8. Sanders BS, Wilcox RB III and Higgins LD: Heterotopic ossification of the deltoid muscle after arthroscopic rotator cuff repair. Am J Orthop (Belle Mead NJ) 39: E67-E71, 2010.
9. Xu Y, Huang M, He W, He C, Chen K, Hou J, Huang M, Jiao Y, Liu R, Zou N, *et al*: Heterotopic Ossification: Clinical features, basic researches, and mechanical stimulations. Front Cell Dev Biol 10: 770931, 2022.
10. Edwards DS, Kuhn KM, Potter BK and Forsberg JA: Heterotopic Ossification: A review of current understanding, treatment, and future. J Orthop Trauma 30 (Suppl 3): S27-S30, 2016.
11. Peake JM, Della Gatta P, Suzuki K and Nieman DC: Cytokine expression and secretion by skeletal muscle cells: Regulatory mechanisms and exercise effects. Exerc Immunol Rev 21: 8-25, 2015.
12. Zhang S, Sun S, He J and Shen L: NT-3 promotes osteogenic differentiation of mouse bone marrow mesenchymal stem cells by regulating the Akt pathway. J Musculoskelet Neuronal Interact 20: 591-599, 2020.

13. Feng H, Xing W, Han Y, Sun J, Kong M, Gao B, Yang Y, Yin Z, Chen X, Zhao Y, *et al*: Tendon-derived cathepsin K-expressing progenitor cells activate Hedgehog signaling to drive heterotopic ossification. J Clin Invest 130: 6354-6365, 2020.
14. Xu R, Hu J, Zhou X and Yang Y: Heterotopic ossification: Mechanistic insights and clinical challenges. Bone 109: 134-142, 2018.
15. Doherty C, Lodyga M, Correa J, Di Ciano-Oliveira C, Plant PJ, Bain JR and Batt J: Utilization of the rat tibial nerve transection model to evaluate cellular and molecular mechanisms underpinning denervation-mediated muscle injury. Int J Mol Sci 25: 1847, 2024.
16. Bertin JSF, Marques MJ, Macedo AB, de Carvalho SC and Neto HS: Effect of photobiomodulation on denervation-induced skeletal muscle atrophy and autophagy: A study in mice. J Manipulative Physiol Ther 45: 97-103, 2022.
17. Rodríguez MP and Cabello-Verrugio C. Soluble factors associated with denervation-induced skeletal muscle atrophy. Curr Protein Pept Sci 25: 189-199, 2024.
18. Komatsu M, Nakada T, Kawagishi H, Kato H and Yamada M: Increase in phospholamban content in mouse skeletal muscle after denervation. J Muscle Res Cell Motil 39: 163-173, 2018.
19. Lee J, Jang SH, Lee SJ and Lee O: Synchrotron radiation imaging analysis of neural damage in mouse soleus muscle. Sci Rep 10: 4555, 2020.
20. Yoshimura A, Ito M, Chikuma S, Akanuma T and Nakatsukasa H: Negative regulation of cytokine signaling in immunity. Cold Spring Harb Perspect Biol 10: a028571, 2018.
21. Zhou P, Zheng T and Zhao B: Cytokine-mediated immunomodulation of osteoclastogenesis. Bone 164: 116540, 2022.
22. Mansurov A, Lauterbach A, Budina E, Alpar AT, Hubbell JA and Ishihara J: Immunoengineering approaches for cytokine therapy. Am J Physiol Cell Physiol 321: C369-C383, 2021.
23. Schaible HG, Del Rosso A and Matucci-Cerinic M: Neurogenic aspects of inflammation. Rheum Dis Clin North Am 31: 77-101, ix, 2005.
24. Salisbury E, Rodenberg E, Sonnet C, Hipp J, Gannon FH, Vadakkan TJ, Dickinson ME, Olmsted-Davis EA and Davis AR: Sensory nerve induced inflammation contributes to heterotopic ossification. J Cell Biochem 112: 2748-2758, 2011.
25. Zhang D, Sliwkowski MX, Mark M, Frantz G, Akita R, Sun Y, Hillan K, Crowley C, Brush J and Godowski PJ: Neuregulin-3 (NRG3): A novel neural tissue-enriched protein that binds and activates ErbB4. Proc Natl Acad Sci USA 94: 9562-9567, 1997.
26. Jullien N, Maudinet A, Leloutre B, Ringe J, Haupl T and Marie PJ: Downregulation of ErbB3 by Wnt3a contributes to wnt-induced osteoblast differentiation in mesenchymal cells. J Cell Biochem 113: 2047-2056, 2012.
27. Achilleos A and Trainor PA: Neural crest stem cells: Discovery, properties and potential for therapy. Cell Res 22: 288-304, 2012.
28. Lazard ZW, Olmsted-Davis EA, Salisbury EA, Gugala Z, Sonnet C, Davis EL, Beal E II, Ubogu EE and Davis AR: Osteoblasts Have a Neural Origin in Heterotopic Ossification. Clin Orthop Relat Res 473: 2790-2806, 2015.
29. Joe AW, Yi L, Natarajan A, Le Grand F, So L, Wang J, Rudnicki MA and Rossi FM: Muscle injury activates resident fibro/adipogenic progenitors that facilitate myogenesis. Nat Cell Biol 12: 153-163, 2010.
30. Helmbacher F and Stricker S: Tissue cross talks governing limb muscle development and regeneration. Semin Cell Dev Biol 104: 14-30, 2020.
31. Contreras O, Rossi FMV and Theret M: Origins, potency, and heterogeneity of skeletal muscle fibro-adipogenic progenitors-time for new definitions. Skelet Muscle 11: 16, 2021.
32. Vallecillo-Garcia P, Orgeur M, Vom Hofe-Schneider S, Stumm J, Kappert V, Ibrahim DM, Börno ST, Hayashi S, Relaix F, Hildebrandt K, *et al*: Odd skipped-related 1 identifies a population of embryonic fibro-adipogenic progenitors regulating myogenesis during limb development. Nat Commun 8: 1218, 2017.
33. Wosczyna MN, Biswas AA, Cogswell CA and Goldhamer DJ: Multipotent progenitors resident in the skeletal muscle interstitium exhibit robust BMP-dependent osteogenic activity and mediate heterotopic ossification. J Bone Miner Res 27: 1004-1017, 2012.
34. Lees-Shepard JB, Yamamoto M, Biswas AA, Stoessel SJ, Nicholas SE, Cogswell CA, Devarakonda PM, Schneider MJ Jr, Cummins SM, Legendre NP, *et al*: Activin-dependent signaling in fibro/adipogenic progenitors causes fibrodysplasia ossificans progressiva. Nat Commun 9: 471, 2018.
35. Eisner C, Cummings M, Johnston G, Tung LW, Groppa E, Chang C and Rossi FM: Murine tissue-resident PDGFRα+ fibro-adipogenic progenitors spontaneously acquire osteogenic phenotype in an altered inflammatory environment. J Bone Miner Res 35: 1525-1534, 2020.
36. Akhter ET, Rotterman TM, English AW and Alvarez FJ: Sciatic nerve cut and repair using fibrin glue in adult mice. Bio Protoc 9: e3363, 2019.
37. Engelman JA, Zejnullahu K, Gale CM, Lifshits E, Gonzales AJ, Shimamura T, Zhao F, Vincent PW, Naumov GN, Bradner JE, *et al*: PF00299804, an irreversible pan-ERBB inhibitor, is effective in lung cancer models with EGFR and ERBB2 mutations that are resistant to gefitinib. Cancer Res 67: 11924-11932, 2007.
38. Kang X, Yang MY, Shi YX, Xie MM, Zhu M, Zheng XL, Zhang CK, Ge ZL, Bian XT, Lv JT, *et al*: Interleukin-15 facilitates muscle regeneration through modulation of fibro/adipogenic progenitors. Cell Commun Signal 16: 42, 2018.
39. Livak KJ and Schmittgen TD. Analysis of relative gene expression data using real-time quantitative PCR and the 2(-Delta Delta C(T)) Method. Methods 25: 402-408, 2001.
40. Zhao SJ, Kong FQ, Jie J, Li Q, Liu H, Xu AD, Yang YQ, Jiang B, Wang DD, Zhou ZQ, *et al*: Macrophage MSR1 promotes BMSC osteogenic differentiation and M2-like polarization by activating PI3K/AKT/GSK3β/β-catenin pathway. Theranostics 10: 17-35, 2020.
41. Pan JM, Wu LG, Cai JW, Wu LT and Liang M: Dexamethasone suppresses osteogenesis of osteoblast via the PI3K/Akt signaling pathway in vitro and in vivo. J Recept Signal Transduct Res 39: 80-86, 2019.
42. Davis EL, Davis AR, Gugala Z and Olmsted-Davis EA: Is heterotopic ossification getting nervous?: The role of the peripheral nervous system in heterotopic ossification. Bone 109: 22-27, 2018.
43. Hwang CD, Pagani CA, Nunez JH, Cherief M, Qin Q, Gomez-Salazar M, Kadaikal B, Kang H, Chowdary AR, Patel N, *et al*: Contemporary perspectives on heterotopic ossification. JCI insight 7: e158996, 2022.
44. Yuasa M, Mignemi NA, Nyman JS, Duvall CL, Schwartz HS, Okawa A, Yoshii T, Bhattacharjee G, Zhao C, Bible JE, *et al*: Fibrinolysis is essential for fracture repair and prevention of heterotopic ossification. J Clin Invest 125: 3117-3131, 2015.
45. Wan QQ, Qin WP, Ma YX, Shen MJ, Li J, Zhang ZB, Chen JH, Tay FR, Niu LN and Jiao K: Crosstalk between bone and nerves within bone. Adv Sci (Weinh) 8: 2003390, 2021.
46. Qureshi AT, Crump EK, Pavey GJ, Hope DN, Forsberg JA and Davis TA: Early characterization of blast-related heterotopic ossification in a rat model. Clin Orthop Relat Res 473: 2831-2839, 2015.
47. Olmsted-Davis EA, Salisbury EA, Hoang D, Davis EL, Lazard Z, Sonnet C, Davis TA, Forsberg JA and Davis AR: Progenitors in peripheral nerves launch heterotopic ossification. Stem Cells Transl Med 6: 1109-1119, 2017.
48. Alfieri KA, Forsberg JA and Potter BK: Blast injuries and heterotopic ossification. Bone Joint Res 1: 192-197, 2012.
49. Smith JK, Miller ME, Carroll CG, Faillace WJ, Nesti LJ, Cawley CM and Landau ME: High-resolution ultrasound in combat-related peripheral nerve injuries. Muscle Nerve 54: 1139-1144, 2016.
50. Edwards DS, Clasper JC and Patel HD: Heterotopic ossification in victims of the London 7/7 bombings. J R Army Med Corps 161: 345-347, 2015.
51. Wang X, Li F, Xie L, Crane J, Zhen G, Mishina Y, Deng R, Gao B, Chen H, Liu S, *et al*: Inhibition of overactive TGF-β attenuates progression of heterotopic ossification in mice. Nat Commun 9: 551,2018.
52. Li L, Jiang Y, Lin H, Shen H, Sohn J, Alexander PG and Tuan RS: Muscle injury promotes heterotopic ossification by stimulating local bone morphogenetic protein-7 production. J Orthop Translat 18: 142-153, 2019.
53. O'Brien EJ, Frank CB, Shrive NG, Hallgrímsson B and Hart DA: Heterotopic mineralization (ossification or calcification) in tendinopathy or following surgical tendon trauma. Int J Exp Pathol 93: 319-331, 2012.
54. Wei X, Nicoletti C and Puri PL: Fibro-Adipogenic Progenitors: Versatile keepers of skeletal muscle homeostasis, beyond the response to myotrauma. Semin Cell Dev Biol 119: 23-31, 2021.
55. Gallardo FS, Cordova-Casanova A, Bock-Pereda A, Rebolledo DL, Ravasio A, Casar JC and Brandan E: Denervation Drives YAP/TAZ activation in muscular fibro/adipogenic progenitors. Int J Mol Sci 24: 5585, 2023.

56. Mejias Rivera L, Shore EM and Mourkioti F: Cellular and molecular mechanisms of heterotopic ossification in fibrodysplasia ossificans progressiva. Biomedicines 12: 779, 2024.
57. Tumolo MR, Panico A, De Donno A, Mincarone P, Leo CG, Guarino R, Bagordo F, Serio F, Idolo A, Grassi T and Sabina S: The expression of microRNAs and exposure to environmental contaminants related to human health: A review. Int J Environ Health Res 32: 332-354, 2022.
58. Fisher MC, Clinton GM, Maihle NJ and Dealy CN: Requirement for ErbB2/ErbB signaling in developing cartilage and bone. Dev Growth Differ 49: 503-513, 2007.
59. Linder M, Hecking M, Glitzner E, Zwerina K, Holcmann M, Bakiri L, Ruocco MG, Tuckermann J, Schett G, Wagner EF and Sibilia M: EGFR controls bone development by negatively regulating mTOR-signaling during osteoblast differentiation. Cell Death Differ 25: 1094-1106, 2018.
60. Shirley M: Dacomitinib: First global approval. Drugs 78: 1947-1953, 2018.
61. Zheng HC: The molecular mechanisms of chemoresistance in cancers. Oncotarget 8: 59950-59964, 2017.